

# Occurrence and origin of carbon dioxide in the Fushan Depression, Beibuwan Basin, South China Sea

Meijun Li<sup>a,\*</sup>, Tieguan Wang<sup>a</sup>, Ju Liu<sup>b</sup>, Hong Lu<sup>c</sup>, Weiqiang Wu<sup>b</sup>, Lihui Gao<sup>b</sup>

<sup>a</sup>Key Laboratory for Hydrocarbon Accumulation Mechanism of the Chinese Ministry of Education, Earth Sciences and Geoinformatics School, China University of Petroleum, Beijing 102200, China

<sup>b</sup>Petro China Southern Oil Exploration and Development Company, Guangzhou 510640, China

<sup>c</sup>Guangzhou Institute of Geochemistry, Chinese Academy of Sciences, Guangzhou 510640, China

Received 21 September 2006; received in revised form 10 May 2007; accepted 9 July 2007

## Abstract

Natural gases produced from the Fushan Depression, Beibuwan Basin, South China Sea are generally rich in carbon dioxide. The  $\delta^{13}\text{C}$  values of methane in these gases are within the range of  $-41.18\text{‰}$  to  $-47.00\text{‰}$ . This, together with the linearity of the  $\delta^{13}\text{C}$  values of methane to butane in the “natural gas plots,” indicates that the hydrocarbon gases are of organic origin. The  $\delta^{13}\text{C}_{\text{CO}_2}$  values of these gases are in the range of  $-5.1\text{‰}$  to  $-7.5\text{‰}$ , suggesting an inorganic origin. A dominant mantle source for the  $\text{CO}_2$  in these gases was determined on the basis of a simple binary mixing model using the  $\delta^{13}\text{C}_{\text{CO}_2}$  values and  $^3\text{He}/^4\text{He}$  ratios of associated helium in these gases. The primary geological controls on the occurrence of  $\text{CO}_2$  rich gas accumulations in the Fushan Depression are discussed following a comparison with other sedimentary basins in the region.

© 2007 Elsevier Ltd. All rights reserved.

**Keywords:** Carbon dioxide; Origin; Natural gas; The South China Sea

## 1. Introduction

This manuscript represents the first attempt in documenting the geological occurrence of carbon dioxide ( $\text{CO}_2$ ) in the Beibuwan Basin, one of the four major Cenozoic basins in the northern continental shelf of the South China Sea region. Located in the southeastern Beibuwan Basin, the Fushan Depression is the focus of the present investigation. Hydrocarbon exploration in this depression began at the end of 1950s, with approximately 70 wells being drilled in the subsequent three decades. Since the early 1990s, a number of commercial oil and gas fields have been discovered in this depression.

The hydrocarbons produced from the Fushan Depression include natural gas, condensate, light oil, crude oil,

and a small amount of heavy oil in shallow-buried pools. The principal gas production consists of hydrocarbon gases with methane dominance, with variable amounts of  $\text{CO}_2$  (Fig. 1). Gas pools with high  $\text{CO}_2$  contents were observed previously in other parts of the South China Sea. In the Yinggehai Basin, for example, the maximum  $\text{CO}_2$  concentrations in some gas pools are up to 94% (e.g. Hao et al., 1996). Gas pools with high content of  $\text{CO}_2$  were also discovered in the Pearl River Mouth (PRMB) and Qiongdongnan basins (e.g. He and Liu, 2004). Based on earlier studies (Chen et al., 2004; He et al., 2004; Huang et al., 2002, 2004; Liu et al., 2004),  $\text{CO}_2$  in the Yinggehai Basin appears to be inorganic in origin, formed from high temperature thermal decomposition of calcareous shales with deep burial in the Tertiary strata and pre-Tertiary carbonates in the basement. In contrast,  $\text{CO}_2$  in the PRMB and Qiongdongnan basins are thought to have a mixed mantle and crustal origin (He et al., 2004; Lai, 1994).

This manuscript reports on the occurrence of  $\text{CO}_2$  in the Fushan Depression and discusses the possible origin of these gases on the basis of stable carbon isotopic

\*Corresponding author. Geological Survey of Canada, 3303-33 Street, NW Calgary, Alberta, Canada T2L 2A7. Tel.: +1 403 2927035; fax: +1 403 2925377 (present); Tel./fax: +86 10 89733422.

E-mail addresses: [meijunli2008@hotmail.com](mailto:meijunli2008@hotmail.com) (M. Li), [wttgg2003@yahoo.com.cn](mailto:wttgg2003@yahoo.com.cn) (T. Wang).

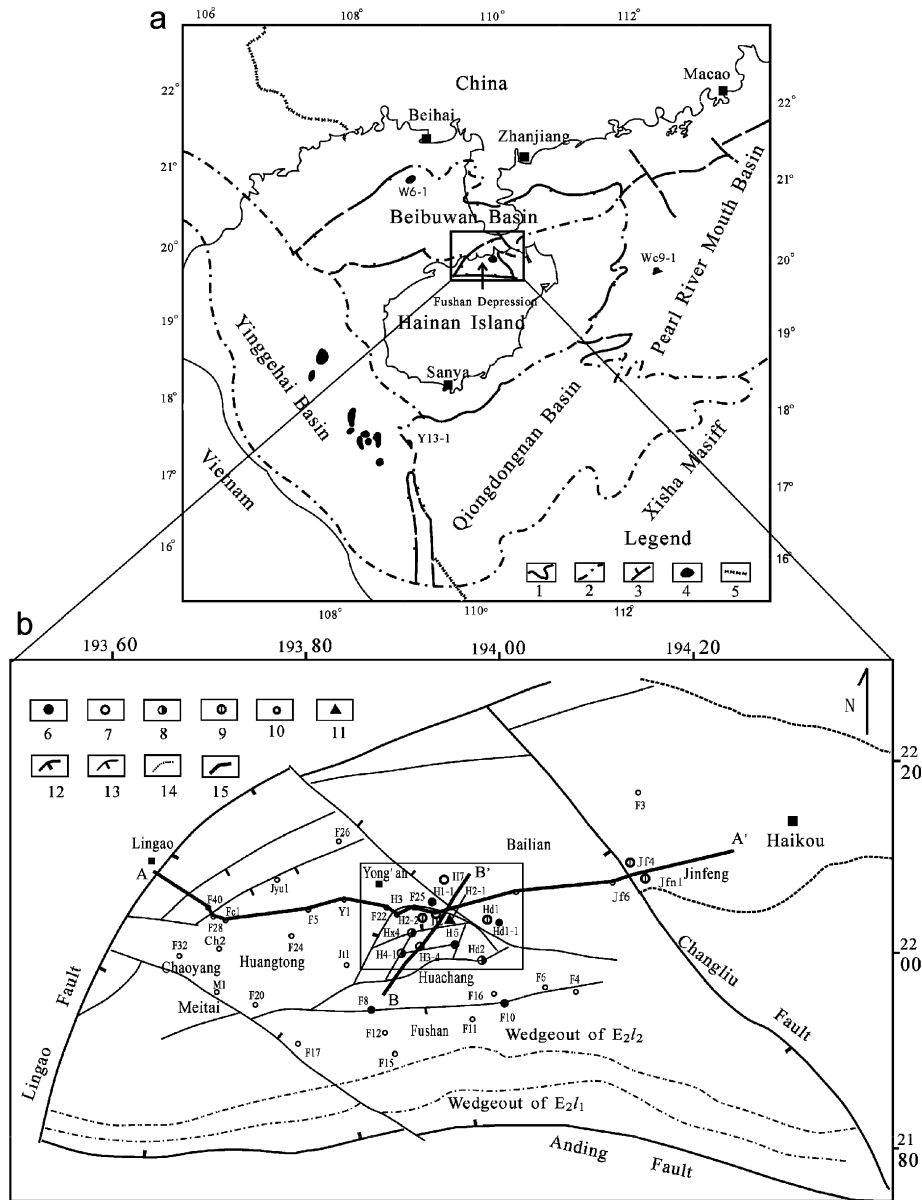


Fig. 1. Maps showing the location and the distribution of the CO<sub>2</sub>-rich gas pools in the Fushan Depression. The insert box in (b) donates the focused study area. Legend: 1—coastline; 2—basin boundary; 3—fault; 4—oil/gas field; 5—national boundary; 6—well with CO<sub>2</sub>>20%; 7—well with CO<sub>2</sub><20%; 8—well sampling (CO<sub>2</sub>>20%); 9—well sampling (CO<sub>2</sub><20%); 10—dry/oil well; 11—well for burial history reconstruction; 12—boundary fault; 13—fault; 14—hypothetical boundary; 15—location of cross-section in Figs. 2 (A-A') and 10 (B-B').

compositions of the CO<sub>2</sub> and associated hydrocarbon gases, as well as the isotopic compositions of helium. Comparison will be made with gases produced from other parts of the South China Sea region, as understanding the origin of the CO<sub>2</sub> is vital for the establishment of petroleum system models in this basin.

## 2. Geological setting and background

Situated north of the Hainan Island and south of the Qiongzhou Strait, the Fushan Depression is one of the many Mesozoic–Cenozoic rifting half-grabens in the northern continental shelf of the South China Sea. This

NE–E trending depression forms the southeastern portion of the Beibuwan Basin (Figs. 1 and 2), filled with over 9000 m of Cenozoic sediments in an area of approximately 3000 km<sup>2</sup>, one-third of which is offshore.

Most of the Cenozoic strata in the Fushan Depression were developed on a basement consisting of the Paleozoic and Mesozoic granites and classic rocks (Chen et al., 1991). The F3 and F4 wells penetrated the Upper Cretaceous prunosus sandstones and mudstones. The F26 well in the depression penetrated the Lower Paleozoic Tuolie Group, which is composed of phyllitic silts and pebbled sandstones (Fig. 3).

Four orogenic events occurring during the late Mesozoic to Neogene (Fig. 3) controlled the tectonic evolution and

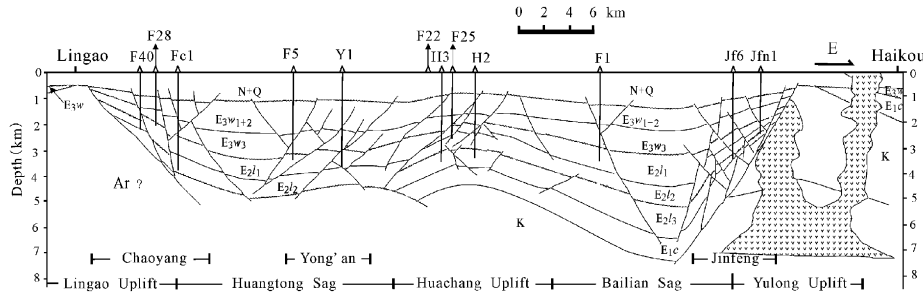


Fig. 2. Cross-section A-A' of the Fushan Depression (see Fig. 1 for the location).

Epoch	Formation	Member	Seismic Horizon	Lithology Column, and source, reservoir, seal assemblage	Lithology description	Tectonic events	Sedimentary environment	Maximum thickness (m) / well	
Quaternary					Sands, Pebbles, Basalt			144.1 / F1	
Neogene	Pliocene	Wanglougang (N <sub>2w</sub> )				Dongsha	Littoral and Neritic	199.5 / F26	
		Dengloujiao (N <sub>1d</sub> )			358.5 / F13				
	Miocene	Jiawei (N <sub>1j</sub> )	T <sub>0</sub>		Predominantly sandstone, interbedded claystone and sandy claystone			573.5 / F1	
		Xiayang (N <sub>1x</sub> )	T <sub>1</sub>					345.5 / F13	
Eogene	Oligocene	Weizhou (E <sub>3w</sub> )	E <sub>3w1</sub>		Interbedded claystone and sand-conglomerate	Nanhai	Lacustrine and littoral	486.0 / F11	
			E <sub>3w2</sub>		Predominantly claystone, interbedded sand-conglomerate			721.0 / F24	
			E <sub>3w3</sub>		Interbedded claystone pebble-sandstone			871 / F5	
			T <sub>2</sub>						
	Eocene	Liushagang (E <sub>2l</sub> )		E <sub>2l1</sub>		Claystone, shale, sandstone, and pebble-sandstone,	Zhuqitong	Shallow lake	766.0 / Y1
				T <sub>5</sub>		Predominantly claystone, shale interbedded sandstone			767.0 / F30
				E <sub>2l2</sub>		Interbedded Claystone, shale, sandstone, and pebble-sandstone		Shallow Lake, and Fan Delta	816.5 / F21
				T <sub>6</sub>					
Paleocene	Changliu (E <sub>1c</sub> )		T <sub>7</sub>		Sand-claystone, clay-sandstone, sand conglomerate, interbedded marlite		Alluvial Fan	710.0 / F19	
			T <sub>8</sub>						
Upper Cretaceous					Claystone, sand-conglomerate, and adesitic porphyrite			771.3 / F3 (unpenetrated)	
Lower Palaeozoic					Phyllitic fine sandstone and pebble-sandstone			126.0 / F26 (unpenetrated)	

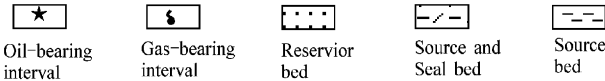


Fig. 3. Generalized stratigraphy and tectonic events of the Fushan Depression.

sedimentary filling of the Beibuwan Basin (e.g. Gong, 1997; Qiu and Gong, 1999). The Late Cretaceous Shenhu orogeny resulted in a number of grabens and half-grabens.

The Paleocene to Eocene Zhuqitong orogeny was the main period of rifting, responsible for the formation of the present Beibuwan basin configuration. In the early rifting

stage, the basin was mainly filled with alluvial and fluvial red pebbled sandstones and mudstones of the Changliu Formation ( $E_{1c}$ ). In the late rifting stage, organic-rich mudstones of the Liushagang Formation ( $E_{2l}$ ) were deposited in a series of well-developed lakes, forming the most important hydrocarbon source rocks in this basin. The Liushagang Formation is the time equivalent of the Wenchang Formation in the PRMB (Zhang et al., 2004; Qiu and Gong, 1999). Major boundary faults occurring in this period controlled the framework of the Fushan Depression. During the late Oligocene Nanhai orogeny, the area was dominated by a shallow lake and swamps, leading to organic-rich mudstones with thin coal interbeds of the Weizhou Formation ( $E_{3w}$ ), the second important source unit in the basin. At the late stage of the Nanhai orogeny, the area was filled with shallow marine deposits, intercalated with fluvial sediments in the second member of the Weizhou Formation. During the Neogene Dongsha orogeny, block faulting dominated the basin evolution. Tectonic movements were usually accompanied by extrusive volcanism, resulted in a series of uplifted and subsided blocks during the deposition of the Jiaowei ( $N_{1j}$ ), Denglujiao ( $N_{1d}$ ) and Wanglougang ( $N_{2w}$ ) formations (Fig. 3).

Volcanic rocks occur widely in the Fushan Depression, as a result of three separate episodes of Cenozoic volcanic activities. Basic extrusive basalts have been encountered in all of the Cenozoic strata. A total of 104 surface craters have been observed. The scenic spot of the Haikou Crater Park is an example of Quaternary crater clusters. The widespread occurrence of subsurface basalts and surface volcanic rocks have severely compromised the quality of seismic data, and impeded the hydrocarbon exploration efforts in the Fushan Depression.

The discovered oil or gas pools from the Fushan Depression mainly occur in the third ( $E_{2l_3}$ ) and first members ( $E_{2l_1}$ ) of the Liushagang Formation. Oils in these pools are dominated by light oil or condensate with an average gravity of 45 ( $^{\circ}$ API). Heavy oils with a gravity of 17–24 ( $^{\circ}$ API) are also discovered in the Oligocene Weizhou Formation ( $E_{3w}$ ).

The Fushan Depression is bounded by the Lingao Fault in the northwest, Anding Fault in the south, and Changliu Fault in the southeast. Major discoveries up to date include light oils and gas condensates in the Huachang uplift and Jinfeng faulted nose structure, and normal gravity oils in the Meitai fault blocks. Other discoveries include the Yong'an and Bohou-Chaoyang oil pools (Fig. 1).

The dark mudstone and shale of the Liushagang Formation in the Huangtong and Bailian sags are thought to be the source rocks of oil and gas in the Fushan Depression. These lacustrine fine-grained rocks account for around 90% of the total rock volume within the Liushagang Formation, with a maximum thickness of 728 m in drilled boreholes and up to 1500 m based on seismic interpretation. According to Ding et al. (2003), these rocks contain on average 1.51% total organic carbon,

with type II and III kerogens. The present burial depth of these rocks exceeds 3000 m, largely within the conventional hydrocarbon generation window. The main petroleum reservoirs in the known discoveries occur in both  $E_{2l_1}$  and  $E_{2l_3}$  sections. The fine-grained sandstone sheets of the fan delta front facies form the main reservoirs in the  $E_{2l_1}$  pools, with an average porosity of 15.5% in the Huachang and Jinfeng oil/gas fields, and 8.8% in the Yong'an, Meitai, and Chaoyang areas. For the  $E_{2l_3}$  pools, coarse sandstones formed in the braided fan delta front are the main reservoir rocks, with an average porosity of 16.8% in the Huachang and Jinfeng oil/gas fields and 13.1% in the other areas. Regional hydrocarbon seals include the 100–500 m of thick lacustrine dark mudstones in the  $E_{2l_2}$  section and the upper  $E_{2l_1}$  to middle  $E_{2l_3}$  sections.

### 3. Samples and methods

Nine gas samples collected from the Huachang and Jinfeng oil and gas fields were used in this study. Sample collection was made from wellheads using 1 L steel cylinders with 2 valves, and the samples were analyzed within 1 month of sample collection. Gas compositions were measured using a HP5890 II gas chromatograph equipped with a thermal conductivity detector, using helium as the carrier gas. The GC oven temperature was set at 80  $^{\circ}$ C and maintained isothermally for 25–30 min. The stable carbon isotopic compositions of gaseous alkanes and  $CO_2$  were analyzed using an offline approach. This involved the isolation of individual components using a gas chromatograph, purification through a glass vacuum tube, combustion to  $CO_2$ , and determination of stable carbon isotopic ratios using a Finnigan MAT-251 mass spectrometer. The analytical precisions for the measured  $\delta^{13}C$  values for  $CO_2$  and  $CH_4$  are within  $\pm 0.02\%$  based on the PDB standard.

The helium isotope compositions were performed in the National Key Laboratory for Gas Geochemistry, Chinese Academy of Sciences (Lanzhou), using a noble gas mass spectrometer (VG5400 VG Isotopes). An inlet system with high vacuum purification line, low leakage, and low background level was used, and the detailed analytical conditions were described by Sun (2001a, b), Sun and Wang (2003).

A total of 24 core and cutting samples were collected from the H2-1 well for vitrinite reflectance measurement. The vitrinite reflectance values ( $\%R_o$ ) were measured on polished rock blocks using a Leica Model MPV-SP microscopic photometer. The BasinMod-1D software developed by the Platte River Associates was used to reconstruct the burial and thermal history of the H2-1 well. Data for modeling were chosen using the formation tops in well completion report, lithologies, and absolute ages given in Qiu and Gong (1999), and erosional thickness determined from well logs and regional geology (Li et al., 2007). The initial porosity, matrix density, thermal conductivity,

and heat capacity were adopted from the default values in the BasinMod-1D. Standard LLNL (Lawrence Livermore National Laboratory) kinetics for Type II and Type III kerogen are used in thermal maturity modeling. The mechanical compaction model was used in the burial history reconstruction. An average geothermal gradient of about 3.0 °C (Kang et al., 1995; Zhang and Wang, 2000) was used, and the value is slightly higher in the Liushagang Formation and deeper strata but lower in the Weizhou Formation and shallower formations. Measured % $R_o$  values were used to constrain and calibrate the thermal history model.

Seven oil reservoir sandstone samples from the E<sub>2</sub>/3 section of the H2-1 well were also collected for hydrocarbon-bearing fluid inclusion investigation and homogenization temperature ( $T_h$ ) measurement. Fluid inclusions were studied using polarized and fluorescent light observation and microthermometry on a Linkam THMS-G600 heating–freezing stage attached to a Leica DMRXHC Petrological Microscope, housed in the Beijing Research Institute of Uranium Geology. Most of the hydrocarbon-bearing fluid inclusions were found in the secondary enlargement of detrital quartzs, and homogenization temperature measurement was made on associated aqueous fluid inclusions, with a total of 136  $T_h$  values being obtained.

In order to evaluate the potential impact of volcanic activities on petroleum fluid compositions, the thickness of basalts in each stratigraphic unit was mapped using wireline logs from 48 boreholes.

## 4. Results and discussion

### 4.1. Gas compositions

The chemical compositions of the natural gases produced from the Fushan Depression are shown in Table 1. While most gases are dominated by methane, their CO<sub>2</sub> contents vary considerably (0.01–97.2%). Gases with the highest CO<sub>2</sub> contents were found from the E<sub>2</sub>/3 gas pool penetrated by the H3-4 well, which has a CO<sub>2</sub> content of around 97.2% and CH<sub>4</sub> accounts for only 0.75%. Natural gases with variable CO<sub>2</sub> contents were also reported in other parts of the South China Sea region (Hao et al., 1996; Huang et al., 2002, 2004). However, the gases produced from the Fushan Depression are distinguished from other gases by displaying relatively high C<sub>2</sub>+ hydrocarbon contents. These compounds account for more than 20% in most of the gases in the Fushan Depression, but less than 4% in gases from the Yinggehai Basin (Hao et al., 1996) and less than 2% from the PRMB and Qiongdongnan basins (e.g. Liu et al., 2004).

Table 1  
The compositions of natural gases from the Fushan Depression

Well	Fm.	Depth (m)	C <sub>1</sub> (%)	C <sub>2</sub> (%)	C <sub>3</sub> (%)	iC <sub>4</sub> (%)	nC <sub>4</sub> (%)	C <sub>5</sub> + (%)	O <sub>2</sub> (%)	N <sub>2</sub> (%)	CO <sub>2</sub> (%)	GOR (m <sup>3</sup> /m <sup>3</sup> )	C <sub>1</sub> /∑C <sub>2</sub> + (%)	Well sampled
<i>Huachang</i>														
H3-4	E <sub>2</sub> /1	2150.0–2153.3	70.4	4.41	8.07	2.79	3.87	4.75	0.70	3.86	1.15	<sup>a</sup>	2.95	
	E <sub>2</sub> /3	3348.0–3355.0	0.75	0.00	0.00	0.00	0.00	0.01	0.42	1.62	97.2	<sup>b</sup>	nd	▲
H5	E <sub>2</sub> /3	2715.8–2731.0	62.7	13.9	6.91	1.29	0.98	1.93	0	0.0	12.29	1370	2.51	
		3008.6–3011.0	7.12	2.17	2.93	0.97	0.34	3.91	0	10.74	71.82	3470	0.69	
HX4	E <sub>2</sub> /3	2965.6–3005.6	49.17	14.60	14.55	3.68	2.04	2.77	0	2.07	11.12	4500	1.31	
		3194.6–3203.6	24.9	8.57	9.36	1.74	2.91	0.71	0.72	3.29	47.8	8350	1.07	▲
HD1	E <sub>2</sub> /3	3329.4–3372.8	66.13	13.91	7.55	1.31	1.27	0.98	1.3	4.5	3.05	1200	2.64	
		3412.6–3422.8	38.35	3.42	0.62	0.08	0.04	0.28	7.03	31.18	19	<sup>a</sup>	8.64	
H1-1	E <sub>2</sub> /3	3347.2–3401.1	67.77	13.87	7.72	2.52	1.39	1.24	0.45	1.43	3.61	<sup>a</sup>	2.53	
		3465.6–3528.5	47.59	10.58	6.29	1.66	1.17	2.43	0.68	2.16	27.44	3690	2.15	
H4-1	E <sub>2</sub> /3	2815.6–2862.2	19.0	5.48	6.61	1.12	2.13	0.7	0.60	2.76	61.6	1880	1.18	▲
HD2	E <sub>2</sub> /3	2542.0–2563.0	35.8	9.26	8.65	1.73	2.70	0.76	0.83	3.67	36.6	620	1.55	▲
H1	E <sub>2</sub> /3	3181.2–3220.6	64.3	17.29	8.44	1.86	1.36	0.56	0.00	1.08	5.11	130	2.18	
H2-2	E <sub>2</sub> /3	2793.0–3021.0	41.58	15.84	17.34	4.07	6.75	1.54	1.60	6.36	4.92	1200	0.91	▲
H2-2 <sup>c</sup>	E <sub>2</sub> /3	2793.0–3021.0	37.43	14.83	17.29	4.25	7.20	1.61	2.62	10.30	4.47	1200	0.83	▲
H7	E <sub>2</sub> /3	3383.2–3493.2	56.70	14.55	12.29	2.16	3.52	6.72	0.32	0.63	3.11	8000	1.44	
<i>Fushan</i>														
F8	E <sub>2</sub> /3	1687.6–1689.0	2.3	1.92	0.33	0.09	0.08	0.8	0	4.10	90.38	nd	0.71	
F10	E <sub>2</sub> /3	1587.8–1600.0	66.1	5.52	3.35	0.54	0.47	0.02	0	3.32	20.68	nd	6.68	
<i>Jinfeng</i>														
JFN1	E <sub>2</sub> /3	2213.5–2216.0	63.75	14.55	10.83	1.87	2.84	0.55	0.39	2.08	3.14	1200	2.08	▲
JF4	E <sub>2</sub> /3	1969.4–1993.4	61.37	15.72	10.90	3.63	3.50	1.02	0.27	1.01	2.58	1000	1.77	▲
JF6	E <sub>2</sub> /3	2734.0–2738.0	74.5	7.62	7.43	2.58	1.33	4.99	0.00	1.15	0.40	70	3.11	

Note: nd = no data.

<sup>a</sup>Light oil pool with a small amount of gas.

<sup>b</sup>Gas pool.

<sup>c</sup>Multiple analysis.

#### 4.2. CO<sub>2</sub> rich gases

Gas pools with high CO<sub>2</sub> contents are distributed in the two areas of the Fushan Depression. One is represented by the F8 and F10 wells along the main boundary fault of the Fushan south slope, and another occurs in the Huachang fault block, including the H3-4, H5, Hx4, H4-1, H1-1, Hd1 and Hd2 wells (Fig. 1 and Table 1). The CO<sub>2</sub> contents are commonly less than 5% in gases from the Jinfeng oil and gas field, whereas gases from the Meitai Oilfield and Yong'an oil-bearing structures are associated gases in normal oil reservoirs.

Known petroleum reservoirs in the Fushan Depression include payzones in the E<sub>2</sub>l<sub>3</sub>, E<sub>2</sub>l<sub>2</sub>, and E<sub>2</sub>l<sub>1</sub> members of the Liushagang Formation and the E<sub>3</sub>w<sub>2</sub> member of the Weizhou Formation. Reservoirs containing high CO<sub>2</sub> gases are limited to the E<sub>2</sub>l<sub>3</sub> member (Table 1). In the H3-4 well, for example, gases produced from the E<sub>2</sub>l<sub>1</sub> reservoirs contain less than 2% CO<sub>2</sub> whereas gases in the E<sub>2</sub>l<sub>3</sub> pools are dominated by CO<sub>2</sub> (>97%). The E<sub>2</sub>l<sub>3</sub> reservoirs usually include these payzones, i.e. upper, middle, and lower units. CO<sub>2</sub> rich gas reservoirs occur mainly in the middle and lower E<sub>2</sub>l<sub>3</sub> units, as shown by the sharp contrast in the chemical compositions of the gases produced from the H5 well. Here, gas produced from the lower E<sub>2</sub>l<sub>3</sub> unit (3008.6–3011.0 m interval) contains about 72% CO<sub>2</sub>, in contrast to a value of only 12% in the upper unit (2715.8–2731.0 m interval).

#### 4.3. Stable carbon isotopes

The isotopic composition of light hydrocarbon gases is controlled kinetically, because <sup>12</sup>C–<sup>12</sup>C bonds are slightly less stable than the <sup>12</sup>C–<sup>13</sup>C bonds (Tang et al., 2000). Thus, hydrocarbon gases that generated by thermal cracking usually show progressive depletion in <sup>13</sup>C from *n*-butane, through propane, ethane to methane (e.g. Clayton, 1991). The hydrocarbon gases with a normal order of the δ<sup>13</sup>C (‰) values (δ<sup>13</sup>C<sub>1</sub> < δ<sup>13</sup>C<sub>2</sub> < δ<sup>13</sup>C<sub>3</sub> < δ<sup>13</sup>C<sub>4</sub>) are considered to be organic in origin, while gases from an inorganic source, mixed inorganic and organic gases, or organic gases with multiple sources can lead to isotopic reversals (e.g. Jenden et al., 1993; Dai, 1992).

As all gas samples from the Fushan Depression show a normal order in the stable carbon isotopes of the gaseous alkanes (Table 2), the δ<sup>13</sup>C values of methane in these gases (−47‰ to −40‰) are also more negative than the empirical cutoff value of −25‰ for inorganic–organic gases (Jenden et al., 1993). Thus, these hydrocarbon gases appear to be organic in origin.

Based on the assumption that gaseous hydrocarbons are formed by thermal cracking of organic matter, and that their carbon isotope ratios are controlled by kinetic isotope effects during formation, Chung et al. (1988) theoretically derived a isotope fractionation equation relative to gaseous hydrocarbons (C<sub>1</sub> to C<sub>5</sub>). It exhibits a line in the carbon isotope composition versus 1/*n* (*n* is the carbon number of gaseous hydrocarbon) plot. This hypothesis was confirmed by laboratory heating experiments. Thus, the relationship among the δ<sup>13</sup>C values of methane to pentane and normal butane (so called “natural gas plot” by Chung et al., 1988) can be used to study the origin and potential mixing of natural gases. As shown in Fig. 4, regardless of their CO<sub>2</sub> contents, the stable carbon isotope values in the Fushan Depression gases approach the linearity in the “natural gas plot.” Thus, it appears undoubtedly that these hydrocarbon gases are principally thermogenic organic gases.

The δ<sup>13</sup>C values of CO<sub>2</sub> in natural gas are known to bear genetic information in resolving organic vs. inorganic derived CO<sub>2</sub>. CO<sub>2</sub> with δ<sup>13</sup>C<sub>CO<sub>2</sub></sub> values in the range of −4‰ to −7‰ is considered to be mantle-derived CO<sub>2</sub> (Clayton et al., 1990; Thrasher and Fleet, 1995). Moore et al. (1977) suggested that CO<sub>2</sub> in fluid inclusions from the Pacific midocean ridge basalt are mantle derived, with the δ<sup>13</sup>C values ranging from −4.5‰ to −6.9‰. It has been shown by Thrasher and Fleet (1995) that the δ<sup>13</sup>C<sub>CO<sub>2</sub></sub> values for large gas accumulations (with over 15 v/v% of CO<sub>2</sub>) are all within the range of −10‰ to 0‰, suggesting an inorganic origin (metamorphic or magmatic). In contrast, the majority of gas accumulations that have less than 10 v/v% CO<sub>2</sub> and low δ<sup>13</sup>C<sub>CO<sub>2</sub></sub> values (<−10‰) have a predominantly organic origin. Dai et al. (1995, 1996, 2005) reviewed the distribution of δ<sup>13</sup>C values of CO<sub>2</sub> in the Chinese sedimentary basins, proposing a δ<sup>13</sup>C value range of organic CO<sub>2</sub> (−10‰ to −30‰) and an inorganic CO<sub>2</sub> range from −8‰ to +3‰. Thus, the δ<sup>13</sup>C values of metamorphic CO<sub>2</sub> derived from carbonate thermal decomposition

Table 2  
The carbon isotopic compositions of CH<sub>4</sub> to C<sub>4</sub>H<sub>10</sub> and CO<sub>2</sub> (‰)

Well	Fm.	Depth (m)	δ <sup>13</sup> C <sub>1</sub>	δ <sup>13</sup> C <sub>2</sub>	δ <sup>13</sup> C <sub>3</sub>	δ <sup>13</sup> C <sub>iC<sub>4</sub></sub>	δ <sup>13</sup> C <sub>nC<sub>4</sub></sub>	δ <sup>13</sup> C <sub>2</sub> −δ <sup>13</sup> C <sub>1</sub>	δ <sup>13</sup> C <sub>CO<sub>2</sub></sub>
H2-2	E <sub>2</sub> l <sub>3</sub>	2793.0–3021.0	−47.00	−33.69	−30.56	−31.93	−29.81	13.31	−7.44
H3-4	E <sub>2</sub> l <sub>3</sub>	3348.0–3355.0	−44.98	−31.69	−30.03	nd	nd	13.29	−5.22
HX4	E <sub>2</sub> l <sub>3</sub>	3194.6–3203.6	−46.10	−32.55	−30.69	−31.44	−30.45	13.55	−5.01
H4-1	E <sub>2</sub> l <sub>3</sub>	2815.6–2862.2	−46.42	−33.68	−30.99	nd	−29.85	12.74	−5.22
HD1	E <sub>2</sub> l <sub>3</sub>	3329.4–3372.8	−45.59	−32.13	−29.24	−29.10	−28.37	13.46	−5.79
HD2	E <sub>2</sub> l <sub>3</sub>	2542.0–2563.0	−43.31	−33.83	−31.37	−30.63	−28.72	9.48	−5.52
JFN1	E <sub>2</sub> l <sub>3</sub>	2213.5–2216.0	−41.18	−31.09	−30.40	−29.25	−29.42	10.09	−10.08
JF4	E <sub>2</sub> l <sub>3</sub>	1969.4–1993.4	−41.93	−30.34	−27.28	−27.20	−25.75	11.59	nd

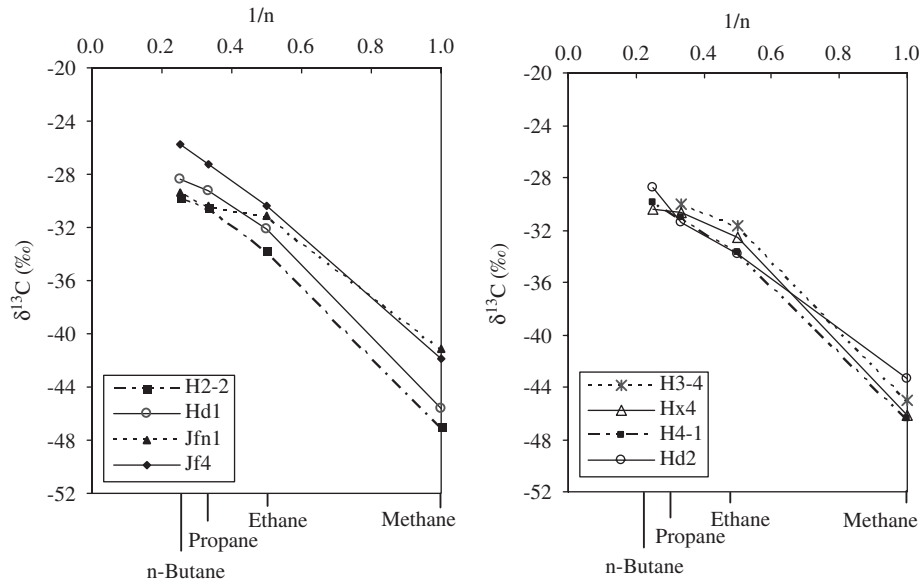


Fig. 4. “Natural gas plots” of gases from the Fushan Depression. (Left: samples with a content of  $\text{CO}_2 < 20\%$ . Right: samples with a content of  $\text{CO}_2 > 20\%$ ).

are close to the mean  $\delta^{13}\text{C}$  values of carbonate rocks ( $0 \pm 3\%$ ), whilst the  $\delta^{13}\text{C}$  values of magmatic and mantle-derived  $\text{CO}_2$  mainly cluster around  $-6 \pm 2\%$ .

$\text{CO}_2$  in all the gas samples we collected from the Fushan Depression except the Jfn1 well show  $\delta^{13}\text{C}_{\text{CO}_2}$  values ranging from  $-7.44\%$  to  $-5.01\%$  (Table 2), indicating an inorganic origin. The samples with less negative carbon isotopic compositions usually have higher concentrations of  $\text{CO}_2$  in the gas, as indicated in Fig. 5. It appears that the  $\delta^{13}\text{C}_{\text{CO}_2}$  in the gases from the Fushan Depression approaches a value of  $-5\%$  when the  $\text{CO}_2$  content is higher than 10% (mol). Similar observations have also been made from other parts of the South China Sea region. In the Yinggehai Basin, for example, reservoirs connected with a diapir usually contain gases with 19–71%  $\text{CO}_2$ , with a  $\delta^{13}\text{C}_{\text{CO}_2}$  values in the range of  $-2\%$  to  $-8\%$  (Huang et al., 2002, 2004). In contrast, reservoirs that are unrelated to the diapirs contain little  $\text{CO}_2$  ( $< 1.5\%$ ), with more negative  $\delta^{13}\text{C}_{\text{CO}_2}$  values ( $-12.10\%$  to  $-18.35\%$ ).

#### 4.4. Helium isotopes

Carbon isotope data do not provide unequivocal interpretations, because average mantle-derived  $\text{CO}_2$  and bulk crustal  $\text{CO}_2$  may have approximately similar values as a result of fluid mixing (e.g. Sherwood-Lollar et al., 1997). However, when stable carbon isotope data are combined with geochemistry of noble gases (helium, neon, and argon) they can be more diagnostic (Wycherley et al., 1999).

In this study, gases with high  $\text{CO}_2$  contents were also analyzed for helium isotopic composition. Measured  $^3\text{He}/^4\text{He}$  ratios are expressed as  $R/R_a$  values by normalizing to the  $^3\text{H}/^4\text{He}$  value for air,  $R_a = 1.4 \times 10^{-6}$ . The  $^3\text{He}/^4\text{He}$  ratios of the gases collected from the H3-4 and H4-1 wells

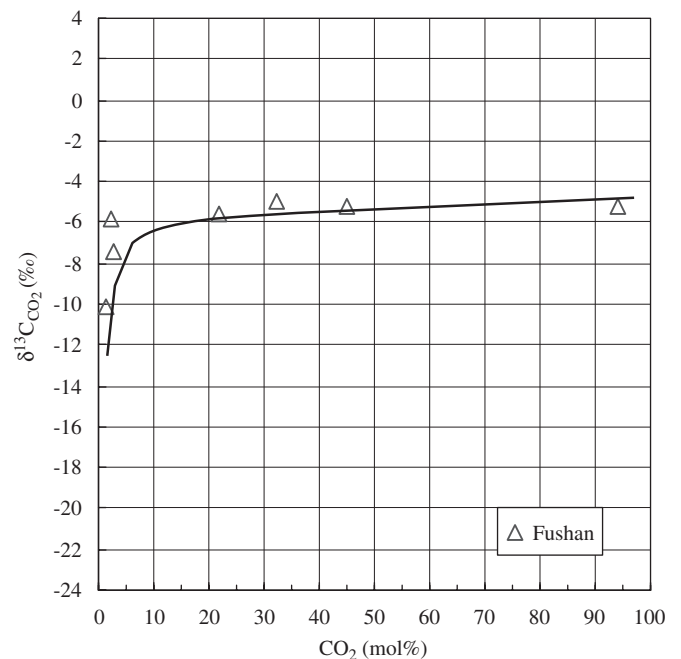


Fig. 5.  $\delta^{13}\text{C}_{\text{CO}_2}$  versus content of  $\text{CO}_2$  (mol%) of gases from the Fushan Depression, Beibuwan Basin.

range  $4.74\text{--}5.03 \times 10^{-6}$ , with the corresponding  $R/R_a$  values of 3.38–3.59.

The  $^3\text{He}/^4\text{He}$  ratio is known to be determined by the crustal production ratios of  $^4\text{He}$  by U and Th decay and  $^3\text{He}$  by a thermal neutron ( $n, \alpha$ ) reaction on  $^6\text{Li}$ . Helium component, typified by the middle oceanic ridge basalts (MORB), is well known to show  $R/R_a = 8 \pm 1$  (e.g. Lupton, 1983). In normal crustal lithologies the radiogenic helium is expected to have an average of  $R/R_a$  at 0.04 (Oxburgh et al., 1986).

The  $R/R_a$  ratios measured from  $\text{CO}_2$  rich gas pools in eastern China range 2.74–4.29 (Dai et al., 1996), indicating that the associated  $\text{CO}_2$  could be mantle derived. In contrast, the  $R/R_a$  ratios in the Qiongdongnan Basin and the LDAB and DFAB regions of the Yinggehai Basin range 0.04–0.54 (He et al., 2004), showing a crustal origin. The  $\delta^{13}\text{C}$  values of  $\text{CO}_2$  in these regions are within the range of  $-7.68\%$  to  $-7.90\%$ , consistent with their inorganic origin.

On the basis of the  $\delta^{13}\text{C}_{\text{CO}_2}$  values and helium gas isotope compositions, it appears conceivable that the  $\text{CO}_2$  in the  $\text{CO}_2$  rich gas pools in the Fushan Depression was mainly mantle derived, with mixing from small amounts of crustal-derived  $\text{CO}_2$ .

#### 4.5. Geological consideration

The tectonic setting and structural styles are known to play a major role in controlling the occurrence of mantle-derived fluids in sedimentary basins. In comparison with the cratonic basins in western and central China, for example, Xu et al. (1995a, b) observed a significant increase in the  $^3\text{He}/^4\text{He}$  ratios in rifting basins in eastern China, especially for gases produced in the vicinity of major fault systems such as the Tanchen-Lujiang Fault Zone. This increase is attributed to the marked occurrence of mantle-derived helium in eastern China due to the thinning of the crust in the rifting basins. Similar relationship was also observed in the Alpine region (Marty et al., 1992), presumably reflecting extensional processes during which melting may easily occur due to upwelling of asthenosphere

and migration into the crust. Polyak and Tolstikhin (1985) have concluded that magmatic/volcanic activity that carries both mantle helium and heat is the principle control for the helium isotopic signatures in the continental crust.

Tectonic configurations of the Fushan depression can be summarized as follows: (1) thinned crust with a Moho buried depth less than 26–28 km (Li et al., 1998; Yan et al., 2006); (2) high geothermal flow, about  $61.2\text{mW/m}^2$  (He et al., 1998; Zhang and Song, 2001; Zhang and Wang, 2000); (3) intensive volcanic activities and widespread occurrence of basalt in Cenozoic formations (e.g. Qiu and Gong, 1999); (4) typical extensional rifting basin with complex fault systems (e.g. Li et al., 1998; Qiu and Gong, 1999). All these tectonic features mentioned above are favorable for the formation and accumulation of mantle-derived  $\text{CO}_2$  in the Fushan Depression.

In the northern Hainan Island and Leizhou Peninsula, the Cenozoic igneous rocks cover an area of more than  $7000\text{km}^2$  (Ho et al., 2000; Yan et al., 2006). Lava flows from the ENE–WSW trending extensional fissure eruptions form thick sequence alternating with other sediments (Yan et al., 2006). The igneous rocks are chiefly basalt. In this study we constructed isopach maps for four stratigraphic intervals to show the sporadic distribution of basalt (also dolerite in the  $\text{E}_2/$  Formation) (Fig. 6). Basalts and dolerite in the  $\text{E}_2/$  Formation mainly occur in the Huachang structure, F8, F10, and F6 well areas. The cumulative thickness of these rocks is 60 m in the F8 well area, but less than 20 m in other areas (Fig. 6A). In the  $\text{E}_3$  strata, limited basalt occurrence was observed mainly in the F10 well area, with a maximum thickness of 160 m

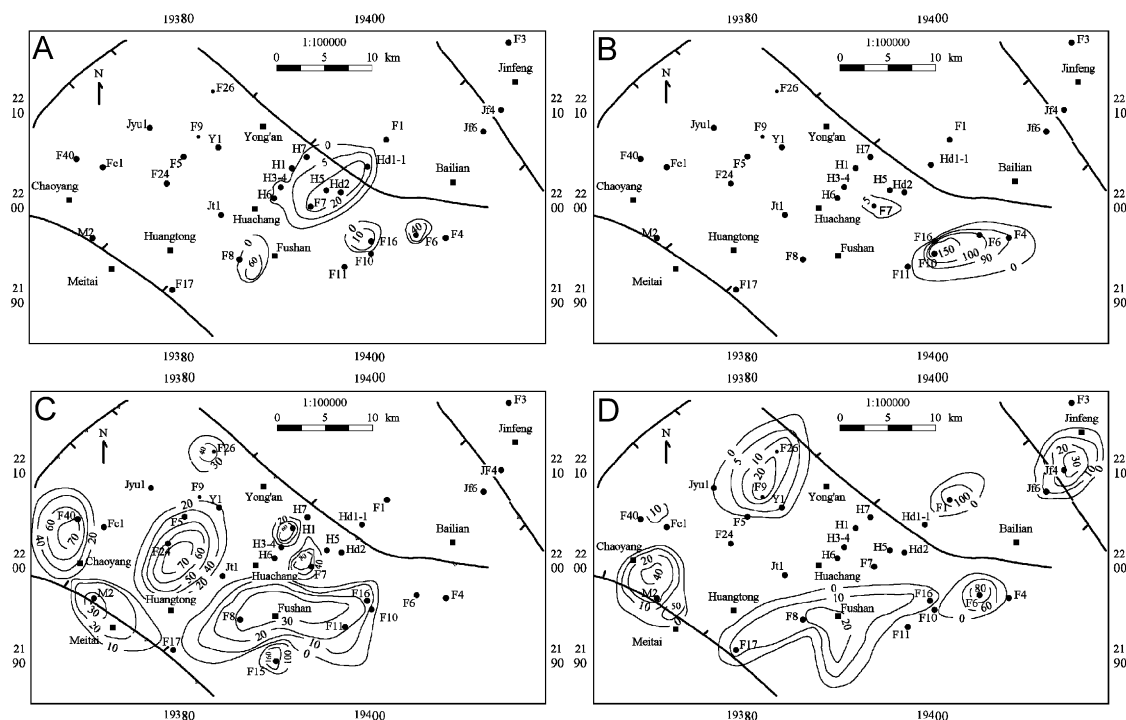


Fig. 6. Contour of basalts in the Fushan Depression (in meters). A: Eocene Liushagang Formation; B: Oligocene Weizhou Formation; C: Neogene; D: Quaternary.

(Fig. 6B). In contrast, igneous rocks occur widely in the Neogene and Quaternary strata (Figs. 6C and D) and have been penetrated in almost all of the major structures, including the Huachang, Meitai, Bohou, Yong'an, and Jinfeng, with a maximum thickness of 80 m. These data may indicate intensified volcanism during the Neogene and Quaternary, consistent with earlier observations (Flower et al., 1992; Ho et al., 2000; Yan et al., 2006). These authors suggest that the main volcanic eruptions occurred during the Pliocene to recent time in the Leizhou Peninsula and Quaternary in the Hainan Island, with relatively low intensities prior to the Pliocene.

The K–Ar ages determined for surface basalts in the study area range 5.9–2.4 Ma (Jia et al., 2003) or 5.6–3.8 Ma (Ho et al., 2000). They were formed by a large-scale magmatic activity associated with the extension of Beibuwan Basin. Major and trace element geochemical characteristics indicate that the basalt may be derived from a uniform mantle source (Jia et al., 2003), and the tectonic conversion from the left lateral shearing to the right lateral shearing of the Red River Fault Zone of about 5 Ma may be responsible for the geodynamic mechanism of mantle abnormal change and magmatic activity (Li et al., 1998). Circumstantial evidence has been reported to relate the volcanism to the activity of deep-seated faults (Ho et al., 2000; Yan et al., 2006).

In order to determine the timing of hydrocarbon and non-hydrocarbon fluid entrapment in the Fushan Depression, the homogenization temperatures of aqueous fluid inclusions associated with hydrocarbon inclusions in the secondary overgrowth of quartz grains were measured

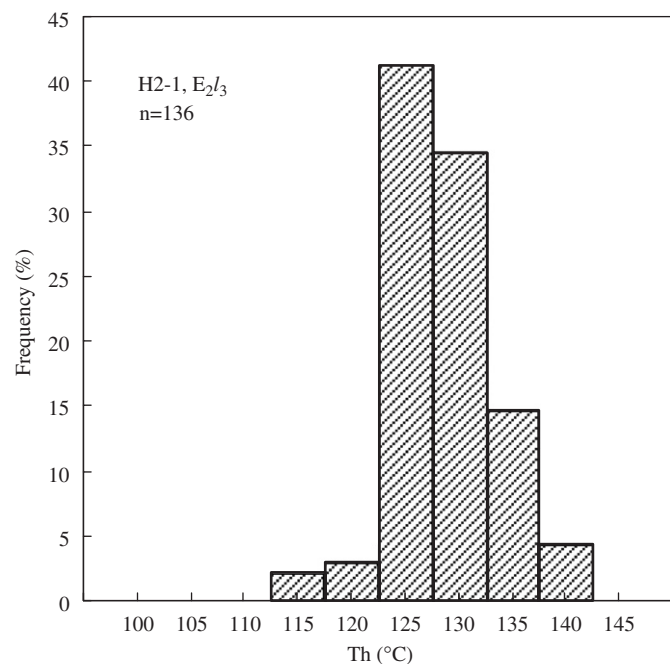


Fig. 7. Histogram of the homogenization temperature of saline water inclusion in the quartz overgrowth from the  $E_2/3$  strata of the H2-1 well. Sampling depth: 2871.0–2942.5 m.

from a number of  $E_2/3$  sandstone reservoir cores of the H2-1 well. The measured Th values range 125–135 °C (Fig. 7). These data were used to constrain the burial and thermal history model reconstructed using the BasinMod-1D package. As shown in Fig. 8, the estimated time for the main hydrocarbon charge in the  $E_2/3$  reservoirs appears to be around the end of mid-Miocene to Pliocene, corresponding to the main stage of magmatic activity in the study area.

It is still unclear what specific roles faults have played in the entrapment and accumulation of  $CO_2$  in the Fushan Depression, even though all known gas pools with high  $CO_2$  content here occur near the main faults (Fig. 9). For example, considerable difference was observed in the  $CO_2$  concentrations in the gases from the  $E_2/1$  and  $E_2/3$  gas reservoirs penetrated by the H3-4 well. As mentioned in Section 4.2, the gases in the  $E_2/1$  reservoirs are dominated by methane, with  $CO_2$  accounting for lesser than 2%. The gases in the  $E_2/3$  reservoirs, in contrast, are dominated by  $CO_2$  (>97%, Table 1). Such gas compositional contrast in different gas reservoirs in the Yinggehai Basin was attributed to the influence of diapirs (Hao et al., 1996). In the Fushan Depression, this may be related to the difference in the connectivity of the two faults systems as shown in Fig. 10. Faults in the “Upper Fault System” occur in the  $E_3w$  and  $E_2/1$  strata and do not cut through the  $E_2/2$  section, whereas faults in the “Lower Fault System” are mostly basement faults cutting through the  $E_2/3$  and terminating in the  $E_2/2$  section (Fig. 10). Thus,  $CO_2$  derived from a deep mantle source can migrate through the Lower Fault System and accumulate in the  $E_2/3$  reservoirs. The thick mudstones in the  $E_2/2$  section serve not only the main petroleum source rocks in the Fushan Depression but also a regional significant fluid barrier for the  $E_2/3$  reservoirs. As a result,  $CO_2$  accumulations occur mainly in the  $E_2/3$  traps, and hydrocarbons in the  $E_2/1$  traps (Fig. 10). The important role of deep seated basement faults in the  $CO_2$  rich gas accumulations in rift basins in eastern China has been discussed by Dai et al. (1996).

#### 4.6. Comparison with $CO_2$ rich gas accumulations in other continent shelf basins of the South China Sea region

In the northern margin of the South China Sea region, Beibuwan Basin has the lowest geothermal flow ( $\sim 61.2$  mW/m<sup>2</sup>, Zhang and Song, 2001; Zhang and Wang, 2000; He et al., 1998). The paleogeothermal gradient of the Beibuwan Basin is estimated to be 3.72 °C/100 m, with the lowest being observed in the Fushan Depression (about 3.0 °C/100 m, Kang et al., 1995; Li et al., 2007). Based on seismic data, the Cenozoic sediments are up to 9000 m near the depocentres of the depression, developed on top of the Paleozoic rocks and Mesozoic granites (Chen et al., 1991). As discussed earlier, the general absence of calcareous shales or carbonates in the deeper strata and the chemical and isotope compositions of the discovered gases indicate a dominantly inorganic mantle source for  $CO_2$  in the Fushan

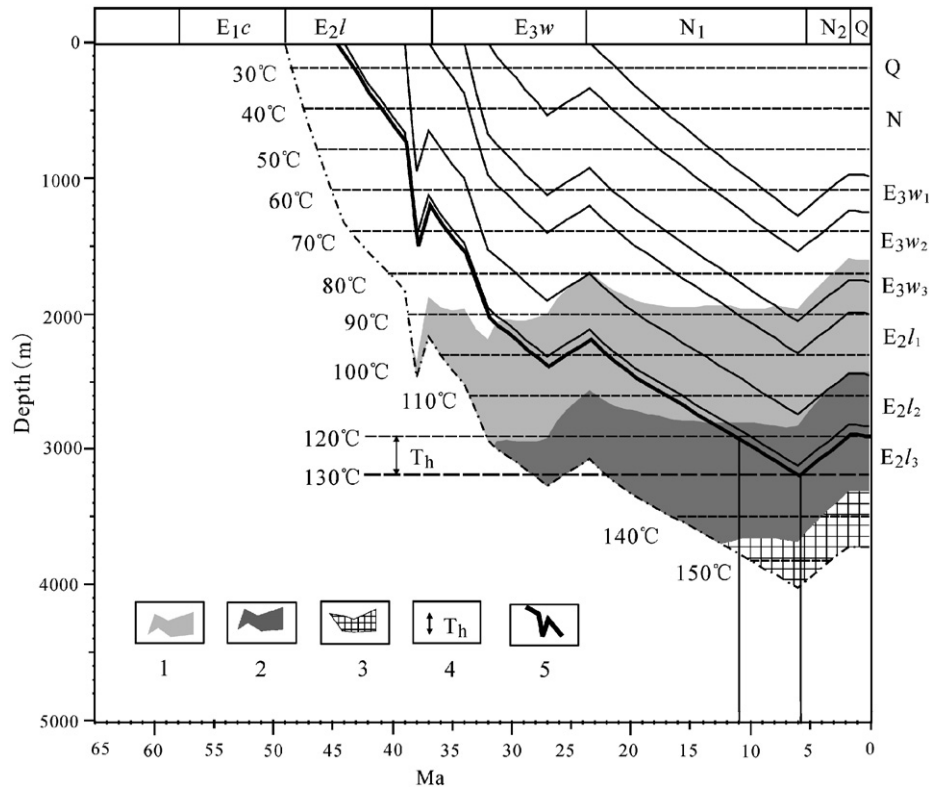


Fig. 8. Buried and thermal history model of the H2-1 well in the Fushan Depression. Combined with homogenization temperature (Fig. 7), the timing of hydrocarbon charging being determined. Legend: 1—early mature; 2—mid mature; 3—late mature; 4—range of homogenization temperature; 5—the buried depth of the fluid inclusion sample.

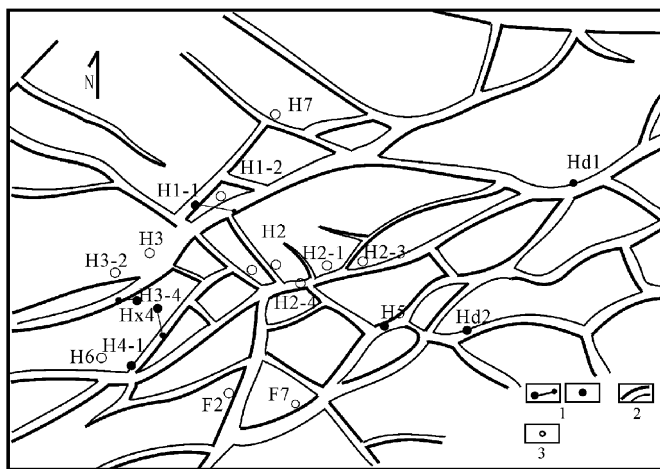


Fig. 9. The top surface structural map of E<sub>2</sub>l<sub>3</sub> of Huachang in Fushan Depression (see Fig. 1 for the location), showing the faults and distribution of wells with high content of CO<sub>2</sub>. Legend: 1—well with CO<sub>2</sub> content >20%; 2—fault; 3—well with CO<sub>2</sub> <20% or oil well with a small amount of gas.

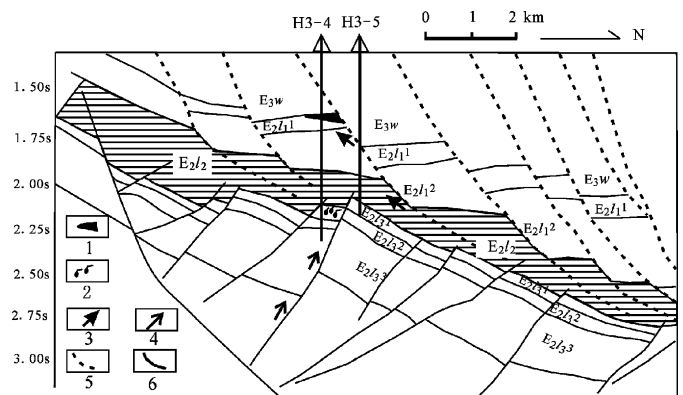


Fig. 10. Cross-section B-B' of the Fushan Depression (see Fig. 1 for the location) showing the fault systems and the accumulation model of CO<sub>2</sub> and hydrocarbon gases in H3-4 well. Legend: 1—oil pool; 2—gas pool; 3—oil migration orientation; 4—gas migration orientation; 5—Upper Fault System; 6—Lower Fault System.

Depression. CO<sub>2</sub>-rich gases observed in the Yinggehai Basin are characterized by  $\delta^{13}\text{C}_{\text{CO}_2}$  values of  $-0.56\text{‰}$  to  $-8.16\text{‰}$  and  $^3\text{He}/^4\text{He}$  ratios in the range of  $0.20\text{--}6.79 \times 10^{-7}$  ( $R/R_a = 0.1\text{--}0.5$ ), indicating a crustal inorganic origin (Hao et al., 1998; Huang et al., 2002,

2004). The calcareous shales in the lower Miocene strata are considered to be the main source of these gases, with only a minor contribution being attributed to the Paleozoic carbonates and/or magmatic activity (Huang et al., 2004). As the Yinggehai Basin has abnormally high paleogeothermal gradients ( $4.25\text{--}4.56\text{ °C}/100\text{ m}$ ) and a rapid heating rate, the lower Miocene calcareous shales could readily reach the threshold temperature (about  $300\text{ °C}$ ) for thermal

decomposition at a burial depth of about 6500 m to generate large volumes of inorganic CO<sub>2</sub> (Huang et al., 2004). The depth of the Moho surface in the Yinggehai basin is about 22 km (Yan and Liu, 2002; Li et al., 1998). In spite of the thin crust, the Cenozoic sediments in the Yinggehai Basin show little evidence of large igneous intrusion, but rather the dominance of shale diapirs (Yan et al., 2006).

Natural gases with high content of CO<sub>2</sub> observed in the PRMB bear similar geochemical characteristics to those of the Fushan Depression (He and Liu, 2004), and these gases appear to be also mantle derived. The similar history of tectonic evolution, sedimentary filling, and magma activities of the Beibuwan and PRMB basins is consistent with the assessment of Li and Rao (1994) and Zhang and Song (2001).

#### 4.7. The mixing model of mantle-derived and organic CO<sub>2</sub>

As the CO<sub>2</sub> rich gas accumulations occur dominantly in sedimentary sequences, it is important to know roughly how much the organic and mantle sources have contributed to the known gas accumulations. Here we provide a preliminary mixing model for explaining the origin of CO<sub>2</sub> in the Fushan Depression.

It is difficult to determine the  $\delta^{13}\text{C}$  value of the organic CO<sub>2</sub> end member, as the breakdown of kerogens gives a wide range of  $\delta^{13}\text{C}$  values (Baker et al., 1995; Clayton, 1995). However, the  $\delta^{13}\text{C}$  value of organic CO<sub>2</sub> can be determined sometimes under relatively geologically restricted conditions. For instance, the average  $\delta^{13}\text{C}_{\text{CO}_2}$  values in the Sichuan and Ordos basins are  $-17.20\text{‰}$  and  $-17.68\text{‰}$ , respectively (Dai et al., 1996). As these basins are tectonically stable with little magmatic activity, the CO<sub>2</sub> in these basins appear to be organic in origin. As shown in Fig. 11, the  $\delta^{13}\text{C}_{\text{CO}_2}$  values in gases from the South China Sea region generally follow the same trends with increasing molar CO<sub>2</sub> content. The lowest  $\delta^{13}\text{C}_{\text{CO}_2}$  value ( $-20.7\text{‰}$ )

came from a gas sample from the Yinggehai Basin that has 0.2 mol% of CO<sub>2</sub> (Fig. 11, right). Thus, the  $\delta^{13}\text{C}$  value of the end member organic CO<sub>2</sub> is assumed to be  $-20\text{‰}$  in our model. The contribution of organic CO<sub>2</sub> is 1% of the total gas when there is no external inorganic CO<sub>2</sub> mixing.

The  $\delta^{13}\text{C}$  value of mantle-derived CO<sub>2</sub> is thought to be  $-4\text{‰}$  to  $-7\text{‰}$  (e.g. Baker et al., 1995; Thrasher and Fleet, 1995; Dai et al., 1996). In the Fushan Depression and Yinggehai Basin, the  $\delta^{13}\text{C}_{\text{CO}_2}$  values gradually approach the value of  $-4\text{‰}$  when the content of CO<sub>2</sub> approaches 100% (Fig. 11, left). Therefore, it is reasonable to assume that the  $\delta^{13}\text{C}$  value of  $-4\text{‰}$  is representative of a mantle-derived CO<sub>2</sub> end member.

Because stable carbon isotope ratios are bulk properties of oil and gas, the  $\delta^{13}\text{C}$  value of mixture involving only two sources can be expressed using a simple binary equation:

$$\delta^{13}\text{C}_{\text{CO}_2} = \delta^{13}\text{C}_A X + \delta^{13}\text{C}_B(1 - X),$$

where  $X$  is the percentage of organic CO<sub>2</sub> in the mixture,  $\delta^{13}\text{C}_A$  and  $\delta^{13}\text{C}_B$  refer to the carbon isotope composition of organic and mantle-derived CO<sub>2</sub>, respectively.

Results of the calculation are shown in Table 3 and Fig. 12. As is expected, the  $\delta^{13}\text{C}_{\text{CO}_2}$  value increases rapidly when the CO<sub>2</sub> content in the gas increase from 1% to 10%, and much less so when the CO<sub>2</sub> content in the gas increases from 10% to 20%. The calculations for gases from the Fushan Depression and PRMB Basin are consistent with the proposition that the CO<sub>2</sub> is mainly mantle derived, whereas some data points from the Yinggehai Basin (Fig. 12) plot away from the expected trend where the CO<sub>2</sub> is thought to be originating from the decomposition of calcareous shales. Although more variables are certainly involved in reality, the simple mixing model presented here clearly gives a good approximation to the possible mixing of organic and mantle-derived CO<sub>2</sub> in the study area. Thus, it appears reasonable to conclude that about 80–93% of the CO<sub>2</sub> discovered in the Fushan Depression is mantle derived.

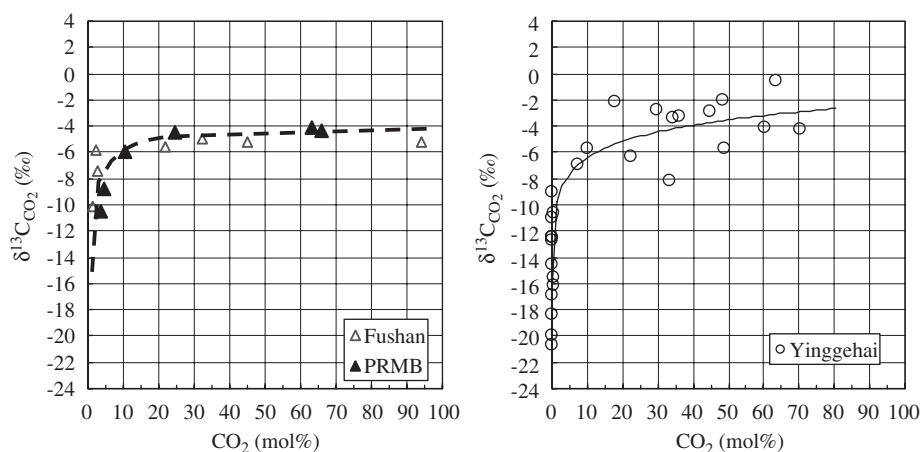


Fig. 11. The relationship between  $\delta^{13}\text{C}_{\text{CO}_2}$  and CO<sub>2</sub> content (mol%). Left: samples from the PRMB (data from He et al., 2004) and the Fushan Depression. Right: samples from the Yinggehai Basin (data from Huang et al., 2004).

Table 3  
The  $^{13}\text{C}_{\text{CO}_2}$  values in mixtures with different proportion of inorganic and organic  $\text{CO}_2$  in the mixing model

$\text{CO}_2$ of total gas (%)	Organic $\text{CO}_2$ of total gas (%)	Inorganic $\text{CO}_2$ of total gas (%)	Organic $\text{CO}_2$ of total $\text{CO}_2$ (%)	Inorganic $\text{CO}_2$ of total $\text{CO}_2$ (%)	$\delta^{13}\text{C}_{\text{CO}_2}$ (‰)
1.00	1.00	0.00	100.00	0.00	-20.00
2.00	0.98	1.02	49.00	51.00	-11.84
3.00	0.97	2.03	32.33	67.67	-9.17
4.00	0.96	3.04	24.00	76.00	-7.84
5.00	0.95	4.05	19.00	81.00	-7.04
6.00	0.94	5.06	15.67	84.33	-6.51
7.00	0.93	6.07	13.29	86.71	-6.13
8.00	0.92	7.08	11.50	88.50	-5.84
9.00	0.91	8.09	10.11	89.89	-5.62
10.00	0.90	9.10	9.00	91.00	-5.44
11.00	0.89	10.11	8.09	91.91	-5.29
12.00	0.88	11.12	7.33	92.67	-5.17
13.00	0.87	12.13	6.69	93.31	-5.07
14.00	0.86	13.14	6.14	93.86	-4.98
15.00	0.85	14.15	5.67	94.33	-4.91
16.00	0.84	15.16	5.25	94.75	-4.84
17.00	0.83	16.17	4.88	95.12	-4.78
18.00	0.82	17.18	4.56	95.44	-4.73
19.00	0.81	18.19	4.26	95.74	-4.68
20.00	0.80	19.20	4.00	96.00	-4.64

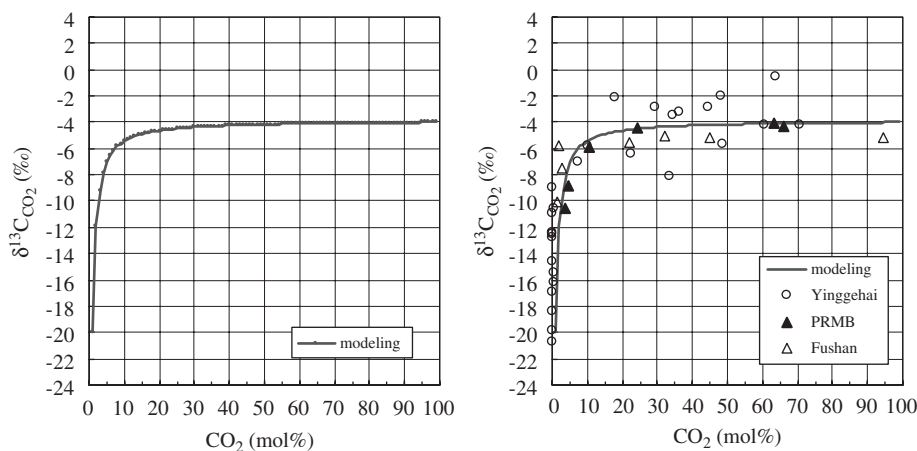


Fig. 12. Left: The relationship between  $^{13}\text{C}_{\text{CO}_2}$  and  $\text{CO}_2$  content (mol%) obtained by mixing modeling. Right: correlation between the mixing model and the data points from the Fushan Depression, the PRMB, and the Yinggehai Basin. Data of the PRMB from He et al. (2004); data of the Yinggehai Basin from Huang et al. (2004).

## 5. Conclusions

Natural gases with high but variable  $\text{CO}_2$  contents were observed in the Fushan Depression, northern continental shelf of the South China Sea region. The gases show  $\delta^{13}\text{C}$  values of methane in the range of  $-41.18\text{‰}$  to  $-47.00\text{‰}$  and a normal  $\delta^{13}\text{C}$  value distribution for  $\text{C}_1$  to  $\text{C}_4$  alkanes, indicating an organic origin, whereas, the  $\delta^{13}\text{C}_{\text{CO}_2}$  values of the gases ( $-5.1\text{‰}$  to  $-7.5\text{‰}$ ) suggest an inorganic origin for the  $\text{CO}_2$ . The  $^3\text{He}/^4\text{He}$  ratios of associated helium in these gases are 3.38–3.59 times the atmospheric ratio, indicating that approximately 42–45% of the helium is mantle derived.

As the Fushan Depression is characterized by thinned crust, intensive volcanic activity, high geothermal flow, and deep seated basement faults, favorable geological conditions exist for the migration and accumulation of mantle-derived  $\text{CO}_2$ . The termination of the deep seated basement faults in the shallow stratigraphic sections and the presence of a regional flow barrier in the  $\text{E}_2/\text{I}_2$  strata appear to be the primary control for the occurrence of  $\text{CO}_2$  versus hydrocarbon rich gas accumulations in the study area. A comparison of the geochemical characteristics of the  $\text{CO}_2$  rich fluids in the study area with other sedimentary basins in the South China Sea region has provided useful information for a better understanding of

the tectonic revolution and sedimentary filling processes of these basins.

### Acknowledgments

The authors would like to thank Dr. Maowen Li of Geological Survey of Canada for his constructive comments and suggestions which significantly improved the quality of this manuscript. This work was financially supported by the Natural Science Foundation of China (Grant no. 40672093) and the ESS-China Hydrocarbon Geosciences Collaboration Project under Natural Resources Canada's International Opportunities Program. We extend our thanks to South Oil Exploration and Development Company of PetroChina for assistance in data and sample collection.

### References

- Baker, J.C., Bai, G.P., Hamilton, P.J., Golding, S.D., Keene, J.B., 1995. Continental-scale magmatic carbon dioxide seepage recorded by dawsonite in the Bowen–Gunnedah–Sydney Basin system, eastern Australia. *Journal of Sedimentary Research* A 65 (3), 522–530.
- Chen, C.P., He, J.X., Yang, J., 2004. A possible lithochemical origin of shallow CO<sub>2</sub> in Yinggehai Basin. *China Offshore Oil and Gas (Geology)* 16 (3), 170–171 (in Chinese).
- Chen, M.X., Xia, S.G., Yang, S.Z., 1991. Local geothermal anomalies and their formation mechanisms on Leizhou Peninsula, Southern China. *Scientia Geologica Sinica* 19 (4), 369–383 (in Chinese).
- Chung, H.M., Gormly, J.R., Squires, R.M., 1988. Origin of gaseous hydrocarbons in subsurface environments: theoretical considerations of carbon isotope distribution. *Chemical Geology* 71, 97–103.
- Clayton, C., 1991. Carbon isotope fractionation during natural gas generation from kerogen. *Marine and Petroleum Geology* 8, 232–240.
- Clayton, C.J., 1995. Controls on the carbon isotope ratio of carbon dioxide in oil and gas fields. In: Grimalt, J.O., Dorronsoro, C. (Eds.), *Organic Geochemistry: Developments and Applications to Energy, Climate, Environment and Human History*, Proceedings of the 17th International Meeting on Organic Geochemistry, San Sebastian, Spain, pp. 1073–1074.
- Clayton, J.L., Spencer, C.W., Koncz, I., Szalay, A., 1990. Origin and migration of hydrocarbon gases and carbon dioxide, Békés Basin, Southeastern Hungary. *Organic Geochemistry* 15 (3), 233–247.
- Dai, J.X., 1992. Identification and distribution of various alkanes gases. *Science in China, Series D, Earth Sciences* 35, 1246–1257.
- Dai, J.X., Song, Y., Dai, C.S., Chen, A.F., Sun, M.L., Liao, Y.S., 1995. The Genetic Features of the Inorganic Gas in East China. Science Press, Beijing, pp. 80–160 (in Chinese).
- Dai, J.X., Song, Y., Dai, C.S., Wang, D.R., 1996. Geochemistry and accumulation of carbon dioxide gases in China. *AAPG Bulletin* 80 (10), 1615–1626.
- Dai, J.X., Yang, S.F., Chen, H.L., Shen, X.H., 2005. Geochemistry and occurrence of inorganic gas accumulations in Chinese sedimentary basins. *Organic Geochemistry* 36 (12), 1664–1688.
- Ding, W.X., Wang, W.J., Ma, Y.J., 2003. Characteristics of Liushagang Formation petroleum system in Fushan Depression of Beibuwan Basin. *Offshore Petroleum* 23 (2), 1–6 (in Chinese).
- Flower, M.F.J., Zhang, M., Chen, C.Y., Tu, K., Xie, G., 1992. Magmatism in the South China basin: 2. Post-spreading quaternary basalts from Hainan Island, South China. *Chemical Geology* 97, 65–87.
- Gong, Z.S., 1997. The Major Oil and Gas Fields of China Offshore. Petroleum Industry Press, Beijing, pp. 199–222 (in Chinese).
- Hao, F., Li, S.T., Zhang, Q.M., 1996. Characteristics and origin of the gas and condensate in the Yinggehai Basin, offshore South China Sea: evidence for effects of overpressure on petroleum generation and migration. *Organic Geochemistry* 24 (3), 363–375.
- Hao, F., Li, S.T., Sun, Y.C., Zhang, Q.M., 1998. Geology, compositional heterogeneities, and geochemical origin of the Yacheng gas field, Qiongdongnan Basin, South China Sea. *AAPG Bulletin* 82 (7), 1372–1384.
- He, J.X., Liu, Q.W., 2004. The analysis and discussion of the characteristics and generative cause, migration and distribution of CO<sub>2</sub> in Ying–Qiong Basins in the north of the South China Sea. *Natural Gas Geosciences* 15 (1), 12–19 (in Chinese).
- He, J.X., Wang, Z.F., Liu, B.M., Zhang, S.L., Zhong, Z.H., 2004. Main control factors of CO<sub>2</sub> reservoir formation in the marginal basins of the north part of South China Sea. *Natural Gas Industry* 24 (9), 19–22 (in Chinese).
- He, L.J., Xiong, L.P., Wang, J.Y., 1998. Geothermal characteristic of South China Sea. *China offshore Oil and Gas (Geology)* 12 (2), 87–90 (in Chinese).
- Ho, K.S., Chen, J.C., Juang, W.S., 2000. Geochronology and geochemistry of late Cenozoic basalts from the Leiqiong area, Southern China. *Journal of Asian Earth Sciences* 18, 307–324.
- Huang, B.J., Xiao, X.M., Dong, W.L., 2002. Multiphase natural gas migration and accumulation and its relationship to diapir structures in the DF1-1 gas field, South China Sea. *Marine and Petroleum Geology* 19, 861–872.
- Huang, B.J., Xiao, X.M., Zhu, W.L., 2004. Geochemistry, origin, and accumulation of CO<sub>2</sub> in natural gases of the Yinggehai Basin, offshore South China Sea. *AAPG Bulletin* 88 (9), 1277–1293.
- Jenden, P.D., Drozan, D.J., Kaplan, I.K., 1993. Mixing of thermogenic natural gases in northern Appalachia Basin. *AAPG Bulletin* 77, 980–998.
- Jia, D.C., Qiu, X.L., Hu, R.Z., Lu, Y., 2003. Geochemical nature of mantle reservoirs and tectonic setting of basalts in Beibu Gulf and its adjacent region. *Journal of Tropical Oceanography* 22 (2), 31–39 (in Chinese).
- Kang, X.D., Li, S.T., Li, Y.L., Hu, Z.L., 1995. The characteristics and thermal evolution of palaeo- and present geothermal field in Beibuwan Basin. *Journal of Changchun Geological College* 25 (2), 173–177 (in Chinese).
- Lai, W.Z., 1994. Origin of carbon dioxide in northern continental shelf, South China Sea. *China Offshore Oil and Gas (Geology)* 8 (5), 319–327 (in Chinese).
- Li, M.J., Wang, T.G., Liu, J., Zhang, M.Z., Lu, H., Ma, Q.L., Gao, L.H., 2007. The discussion on the study of timing and episodes of hydrocarbon charge by fluid inclusion homogenization and burial history—the Fushan Depression as a case. *Oil and Gas Geology* 28 (2), 151–158 (in Chinese).
- Li, P.L., Rao, C.T., 1994. Tectonic characteristics and evolution history of the Pearl River Mouth Basin. *Tectonophysics* 235, 13–25.
- Li, S.T., Lin, C.S., Zhang, Q.M., Yang, S.G., Wu, P.K., 1998. Episodic rifting of continental marginal basins and tectonic events since 10 Ma in the South China Sea. *Chinese Science Bulletin* 43 (8), 797–810 (in Chinese).
- Liu, B.M., Xia, B., Liu, X.X., Zhang, M.Q., Chen, Z.H., 2004. The genetic mechanism of CO<sub>2</sub> in east China and the south western China Sea. *Bulletin of Mineralogy, Petrology and Geochemistry* 23 (3), 207–212 (in Chinese).
- Lupton, J.E., 1983. Terrestrial inert gases: isotope tracer studies and clues to primordial components in the mantle. *A Review of Earth Planet Sciences* 11, 371–414.
- Marty, B., O'Nions, R.K., Oxburgh, E.R., Martel, D., Lombardi, S., 1992. Helium isotopes in Alpine regions. *Tectonophysics* 206, 71–78.
- Moore, J.G., Bachlader, N., Cunningham, C.G., 1977. CO<sub>2</sub>-filled vesicle in mid-ocean basalt. *Journal of Volcano Geothermal Research* 2, 309–327.
- Oxburgh, E.R., O'Nions, R.K., Hill, R.I., 1986. Helium isotopes in sedimentary basins. *Nature* 324, 632–635.

- Polyak, B.G., Tolstikhin, I.N., 1985. Isotopic composition of the earth's helium and the problem of the motive forces of tectogenesis. *Chemical Geology (Isotope Geosciences Section)* 52, 9–33.
- Qiu, Z.J., Gong, Z.S., 1999. *Oil Exploration in China* (vol. 4), Offshore. Geological Publishing House and Petroleum Industry Publishing House, Beijing.
- Sherwood-Lollar, B., Ballentine, C.J., O'Nions, R.K., 1997. The fate of mantle-derived carbon in a continental sedimentary basin: integration of C/He relationships and stable isotopic signatures. *Geochimica et Cosmochimica Acta* 61 (11), 2295–2307.
- Sun, M.L., 2001a. Measurement technology of noble gas isotopes in natural gases. *Acta Sedimentologica Sinica* 19 (2), 271–275 (in Chinese).
- Sun, M.L., 2001b. A new technique for measuring argon isotope in natural gas. *Petroleum Geology and Experiment* 23 (4), 452–456 (in Chinese).
- Sun, M.L., Wang, Z.L., 2003. Comparison and discussion of measurement results for noble gas in natural gas. *Journal of Chinese Mass Spectrometry Society* 24 (2), 377–380 (in Chinese).
- Tang, Y.C., Perry, J.K., Jenden, P.D., Schoell, M., 2000. Mathematical modeling of stable carbon isotope ratios in natural gases. *Geochimica et Cosmochimica Acta* 64, 2673–2687.
- Thrasher, J., Fleet, A.J., 1995. Predicting the risk of carbon dioxide pollution in petroleum reservoirs. In: Grimalt, J.O., Dorronsoro, C. (Eds.), *Organic Geochemistry: Developments and Applications to Energy, Climate, Environment and Human History*, Proceedings of the 17th International Meeting on Organic Geochemistry, San Sebastian, Spain, pp. 1086–1088.
- Wycherley, H., Fleet, A., Shaw, H., 1999. Some observations on the origins of large volumes of carbon dioxide accumulations in sedimentary basins. *Marine and Petroleum Geology* 16, 489–494.
- Xu, S., Nakai, S., Wakita, H., Wang, X.B., 1995a. Mantle-derived noble gases in natural gases from Songliao Basin, China. *Geochimica et Cosmochimica Acta* 59 (22), 4675–4683.
- Xu, S., Nakai, S., Wakita, H., Xu, Y.C., Wang, X.B., 1995b. Helium isotope compositions in sedimentary basins in China. *Applied Geochemistry* 10, 643–656.
- Yan, P., Liu, H., 2002. Analysis on deep crust sounding results in northern margin of South China Sea. *Journal of Tropical Oceanology* 21 (4), 1–12 (in Chinese).
- Yan, P., Deng, H., Liu, H.L., Zhang, Z.R., Jiang, Y.K., 2006. The temporal and spatial distribution of volcanism in the South China Sea region. *Journal of Asian Earth Sciences* 27, 647–659.
- Zhang, C.M., Li, S.T., Yang, J.M., Yang, S.K., Wang, J.R., 2004. Petroleum migration and mixing in the Pearl River Mouth Basin, South China Sea. *Marine and Petroleum Geology* 21, 215–224.
- Zhang, J., Song, H.B., 2001. The thermal structure of main sedimentary basins in the northern margin of the South China Sea. *Journal of Geomechanics* 7 (3), 238–244 (in Chinese).
- Zhang, J., Wang, J.Y., 2000. The deep geothermal characteristics of marginal region of the north part of South China Sea. *Chinese Science Bulletin* 45 (10), 1095–1099 (in Chinese).